1st International Conference on Sensing Technology
November 21-23, 2005 Palmerston North, New Zealand

Hydrogen gas sensor utilizing a high proton affinity of *p*-diketodipyridylpyrrolopyrrole

H. Takahashi* , T. Imoda** and J. Mizuguchi**
* Toyo Ink Engineering Co. Ltd. , **Yokohama National University, Japan
mizu-j@ynu.ac.jp

Abstract

A high-performance hydrogen gas sensor has been developed that utilizes a proton affinity of 1,4-diketo-3,6-bis-(4'-pyridyl)-pyrrolo-[3,4-*c*]-pyrrole (DPPP) known as a red pigment. We found that the N atom of the pyridyl ring of the DPPP can easily be protonated by protons dissociated from H_2 to induce a remarkable change in electrical conductivity by several orders of magnitude. The appealing feature of the device is the reversible operation at room temperature as characterized by a change in electrical resistivity by two orders of magnitude even under 0.05 % H_2.

Keywords: hydrogen gas sensor, diketopyrrolopyrrole, crystal structure

1 Introduction

1,4-Diketo-3,6-diphenyl-pyrrolo-[3,4-*c*]-pyrrole (DPP: Fig. 1(a)) and its derivatives are industrially important red pigments used as colorants in painting industries as well as in imaging areas.[1] Among these, a derivative with pyridyl rings (DPPP: diketodipyridylpyrrolopyrrole; Fig. 1(b)) is known to exhibit a high tinctorial strength of the red color in powders and possesses a high weatherfastness. However, the color suddenly changes from vivid red to dull red when a pigment-dispersed layer in polymers was prepared at elevated temperatures. Our in-depth study clarified that traces of protons are liberated from the polymer matrix at high temperatures and then protonates DPPP at the N atom of the pyridyl ring.[2]

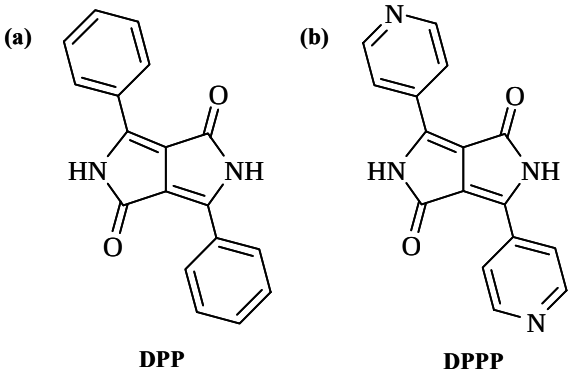

Fig. 1: Molecular conformation: (a) DPP and (b) DPPP.

Our model experiment based on the vapor of nitric acid shows the spectral change as shown in Fig. 2(a).[2] To our great surprise, the electrical resistivity decreases remarkably due to protonation by five orders of magnitude (Fig. 2(b)), also accompanied by the appearance of photoconduction. On the basis of the present outstanding effect, we firmly believed that we could develop a sensitive, H_2-sensor by making use of a high proton affinity of DPPP. Then, our attention was focused on how to dissociate H_2 into protons. We have solved this problem by incorporating Pd or Pt layers into the sensor element. The H_2 sensor which we have successfully developed operates at room temperature in the following sequence: the first step is the dissociation of H_2 by means of a sputtered Pd-layer. The second sequence involves proton capture by the N atom of the pyridyl ring (proton acceptor) that releases an electron, leading to the changes in electrical conductivity.

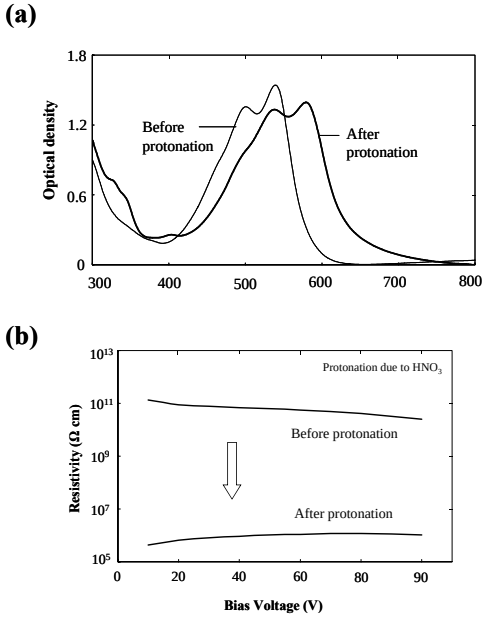

Fig. 2: (a) Absorption spectra and (b) change in resistivity before and after protonation.

2 Experiment

2.1 Operation principle of the H_2 sensor[3]

Fig. 3(a) shows the interdigital electrodes made of Al or ITO (Indium-Tin-Oxide) which were prepared by lithographic technique. The sensor based on the interdigital electrodes must include two important functions: one is to dissociate H_2 into protons and the other is to detect the change in electrical conductivity due to protonation. In order to dissociate H_2, we incorporate a thin layer of Pd, Pt, or Pd/Pt since H_2 is known to be unstable on these metals. At the same time, we apply a rather high electric field between electrodes in order to assist the dissociation of H_2. The successful result is obtained by sputtering Pd or Pt directly on the interdigital electrodes to avoid their contacts in the form of islands as shown in Fig. 3(b), followed by application of DPPP by vacuum evaporation. Since H_2 is fist adsorbed on the surface of DPPP and its subsequent dissociation follows underneath the DPPP layer due to Pd, the DPPP layer must be thin enough to detect the change in electrical conductivity due to protonation. The optimum thickness of Pd layer is about 3 Å while DPPP is deposited to the thickness of 300 - 400 Å.

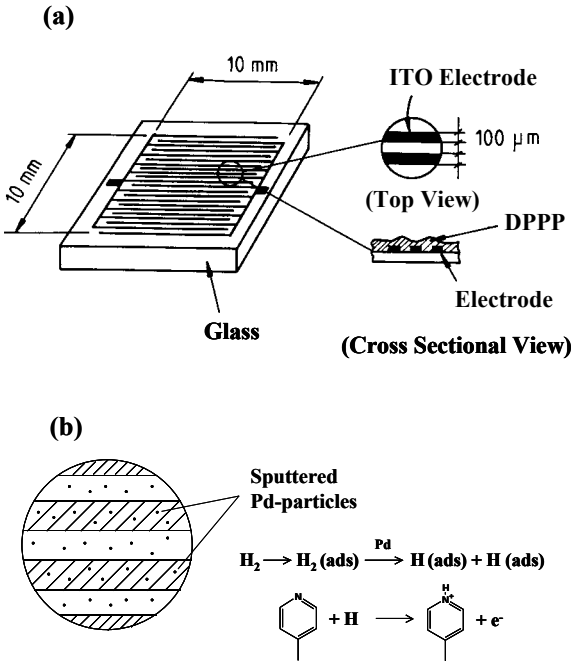

Fig. 3: (a) Interdigital electrodes and (b)magnified Pd-sputtered electrodes.

Al and ITO work equally good as the electrode. Furthermore, no significant difference is recognized in dissociation ability of H_2 between Pd, Pt, and Pd/Pt. Therefore, in the present report, the result is given for the device which includes ITO electrode used in combination with sputtered Pd. The device structure is ITO/sputtered-Pd/DPPP/ITO on the basis of the interdigital electrodes (Fig. 3).

2.2 Synthesis and crystal phase used for the sensor

There are two crystal modifications in DPPP: phase I (grown from vapor phase)[4] and phase II (recrystallized from solution).[5] The projection of the crystal structure onto the molecular plane is shown in Fig. 4 for phases I and II. A striking difference is recognized between two modifications in the hydrogen bond network. Phase I is uniquely characterized by NH···O intermolecular hydrogen bonds between the NH group of one molecule and the O atom of the neighboring one. On the other hand, there exists another type of NH···N hydrogen bonds in phase II in addition to the NH···O bond. This NH···N bond is formed between the NH group of one molecule and the N atom of the pyridyl ring of the neighboring one. In phase I, two N atoms of the pyridyl ring remain free (*i.e.* unbonded) while one of the N atom is blocked by the NH···N hydrogen bond in phase II.

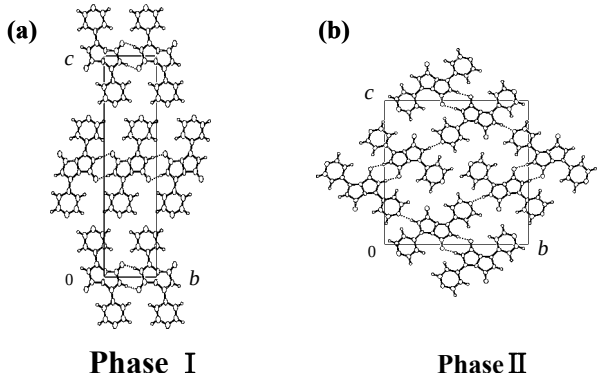

Fig. 4: Projection of the crystal structure.

Therefore, phase I is obviously more appropriate for H_2 sensors because two N atoms are available as the proton acceptor. Luckily enough, phase I is the phase as obtained by vacuum evaporation.

3 Results and Discussion

3.1 3.1 Performance of the H_2 gas sensor

Fig. 5 shows the change in resistivity of the sensor as a function of bias voltage when the sensor is exposed to 100% H_2. The resistivity decreases drastically by three orders of magnitude at room temperature. The resistivities for the H_2 concentrations of 0.05, 0.1, 1 and 10 % are shown in Fig. 6. It is remarkable to note that the resistivity diminishes by two orders of magnitude even for the H_2 concentration of 0.05 %. Furthermore, the resistivity is found to decrease

linearly with increasing H_2 concentration, since Fig. 6 is a log-log plot of the resistivity and H_2 concentration. Fig. 7 shows the build-up of the sensor signals as a function of time. The build-up time (80% of the maximum value) is about 400 ms where the gain is *ca* 900.

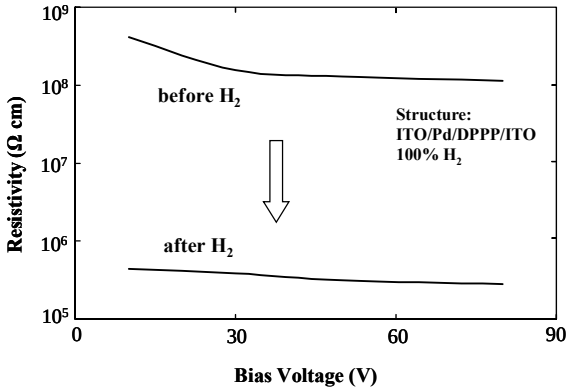

Fig. 5: Change in resistivity of the sensor.

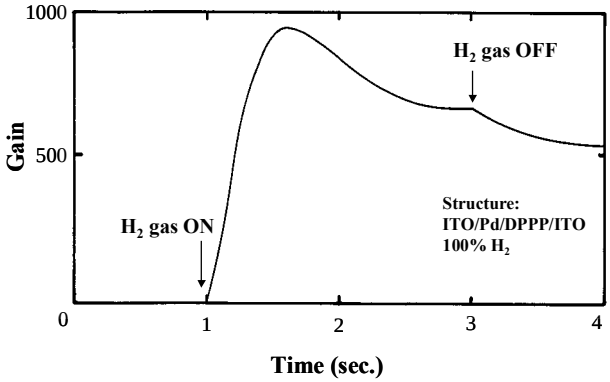

Fig. 6: Log-Log plot of the resistivity and H_2 concentration.

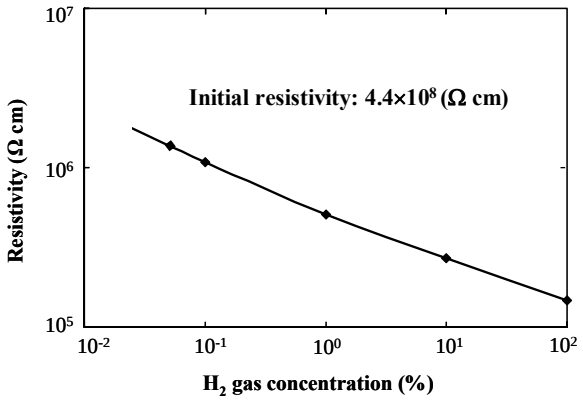

Fig. 7: Build-up of the sensor signal as a function of time.

This indicates that the response is quite rapid in the gain range of several factors. The signal builds up and builds down and then remains nearly constant. When H_2 is switched off, the signal decays and comes back to the initial state in five minutes. The return process is rather slow, but is still reversible a high sensitivity.

3.2 Determination of charge carriers

In general, carrier determination in highly resistive materials is not an easy task because the number of charge carriers is quite small. Organic pigments such as DPPP falls in this category that has a resistivity of about 1011 Ωcm. For these materials, a thermoelectric power method based on the Seebeck effect is sometimes helpful. Fig. 8 shows the experimental setup for the determination of charge carriers on the basis of the Seebeck effect. A soldering rod was used as the heating element as well as the counter electrode to measure thermoelectromotive force that appears due to a temperature difference between two electrodes through DPPP.

An *n*-type Si chip was used as the reference. If the potential at the soldering rod appears positive, the charge carrier is then determined to be electrons. On the contrary, the carrier is holes if the potential is negative. Three kinds of samples were prepared: evaporated DPPP, evaporated/protonated DPPP and H_2 gas sensor based on DPPP. The evaporated/protonated DPPP serves as a model substance for the H_2 gas sensor.

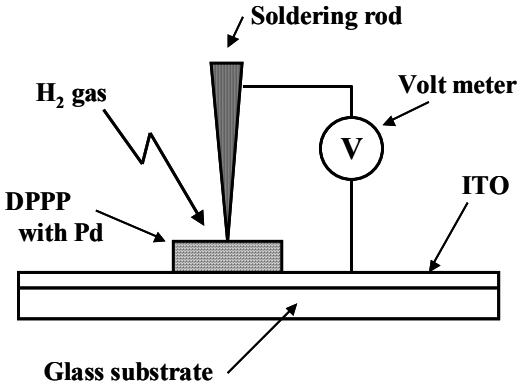

Fig. 8: Experimental setup for measurements of the Seebeck coefficient.

Fig. 9 shows the thermoelectric power *vs* time for DPPP alone, protonated DPPP as well as H_2 gas sensor under 100 % H_2. The magnitude of the signals depends largely on the geometry of the samples (see Experiment). A positive potential appears in all samples at the hot end, indicating clearly that the charge carriers are attributed to electrons. Although the thermoelectric power in H_2 gas sensor is small, it is evident that the potential is positive at the hot end and that the charge carriers are again due to electrons. The present result directly bears out the operation principle shown in Fig. 3.

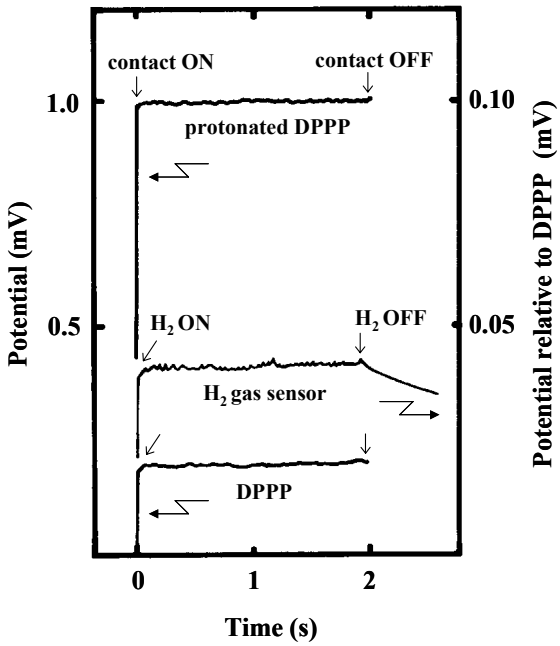

Fig. 9: Themoelectric power observed along the direction of the temperature gradient: evaporated DPPP, evaporated/protonated DPPP and H_2 gas sensor (see text) under 100 % H_2. The potential for the H_2 gas sensor is plotted relative to DPPP. The positive potential always appear in all samples at the hot end, indicating an electron conduction.

3.3 Influence of various gases on the gas sensor

We have studied the influence of various gases on the sensing characteristic: CH_4 (1 %), CO (2 %), CO_2 (24 %), NO (0.6 %) and SO_2 (0.2 %) and H_2O moisture. The sensor was exposed to these gases with a flow rate of 2 l/min. No noticeable effect (*i.e.* less than 0.1 % in resistivity change) was recognized for these gases, indicating that the sensors are free from the influence of ambient gases.

4 Conclusions

A high-performance H_2 gas sensor has been developed on the basis of diketodipyridylpyrrolopyrrole derivatives. The sensing operation involves proton capture by DPPP which releases an electron, leading to the changes in the electrical resistivity. A reduction of resistivity by two orders of magnitude is achieved at room temperature for 0.05 % H_2. The process is reversible and the response time is about 400 ms.

Furthermore, no noticeable effect of ambient gases (CH_4, CO, CO_2, NO and SO_2 gases together with H_2O moisture) is found on the present sensor.

5 References

[1] M. Herbst and K. Hunger, *Industrial Organic Pigments*, pp.550-553, VCH, Weinheim, (1993).

[2] J. Mizuguchi: "Solution and solid state properties of 1,4-diketo-3,6-bis-(4'-pyridyl)-pyrrolo-[3,4-*c*]-pyrrole on protonation and deprotonation", *Ber. Bunsenges. Phys. Chem.*, **97**, 684 (1993).

[3] H. Takahashi and J. Mizuguchi: "Hydrogen gas sensor utilizing a high proton affinity of pyrrolopyrrole derivatives", *J. Electrochem. Soc.* **152**, H69 (2005).

[4] J. Mizuguchi, T. Imoda, H. Takahashi and H. Yamakami: "Polymorph of 1,4-diketo-3,6-bis – (4'-dipyridyl)-pyrrolo-[3,4-*c*]-pyrrole and their hydrogen bond network: A material for H_2 gas sensor" , *Dyes and Pigments*, **68**, 47 (2005).

[5] J. Mizuguchi, H. Takahashi and H. Yamakami: "Crystal structure of 3,6-bis(4'-pyridyl)-pyrrolo [3,4-*c*]-pyrrole-1,4-dione, $C_{16}H_{10}N_4O_2$ at 93K", *Z. Kristallogr. NCS*, **217**, 519 (2002).